A Movement-Tremors Recorder for Patients of Neurodegenerative Diseases

A Movement-Tremors Recorder for Patients of Neurodegenerative Diseases

Abstract
Neurodegenerative diseases such as Alzheimer, Parkinson, motor neuron, and Chorea affect millions of people today. Their effect on the central nervous system causes the loss of brain functions as well as motor disturbances and sometimes cognitive deficits. In such a scenario, the monitoring and evaluation of early symptoms are mandatory for the improvement of the patient's quality of life. Here, the authors describe the development, the laboratory calibration, and the “in-field validation” under the medical supervision of a movement tremors recorder for subjects affected by neurodegenerative diseases. The developed device is based on an array of four accelerometers connected to an embedded development board. This system is able to monitor tremor/movement, accidental falls, and, moreover, it can track the Alzheimer subjects' geographical position. A remote supervisor can collect data from the system through Bluetooth, Wi-Fi, or GSM connections. A data compression algorithm was developed directly on board in order to increase the efficiency of data transmission and reduce power consumptions.

Introduction

In the latest few years, academic and industrial research activities brought to an increasing number and typologies of smart wearable systems available in the market. In such a context, systems for wellness and health monitoring have grown of interest. This technological process is focusing on the wearable application for security and health monitoring. For instance, the number of bracelet locators used by law enforcement agencies is increasing as well as the number of portable devices required by health authorities [1]. Wearable devices have many applications spanning from security to home care fields, and they can be employed in both the indoor and outdoor scenarios. A wide variety of models and devices can be found in applications for fitness trackers and smartwatches employed in conjunction with smartphones. These devices must fulfill several specifications in terms of lightweight, long-term stability, low power consumption, functions, and services. Recently, the increasing performance of these devices is bringing a corresponding increase in biomedical application solutions.

Neurodegenerative diseases, such as Alzheimer, Parkinson, and Chorea, affect millions of people worldwide. They affect the central nervous system killing the neuronal cells. The exact etiology is not still clear, but scientists now recognize that both the genetic and environment contributes play a key role in such diseases. The neural deterioration affects different body activities: equilibrium, speaking, breathing, and heart function. It may also cause cognitive deficits, dementia, and behavioral disorders.

Under this scenario, monitoring systems able to detect early symptoms can be useful for the disease progress [2]; different approaches are described in [3]–[4][5][6]. A wearable measurement system can be used to monitor tremor [7], [8], posture [9], [10], and the so-called “freezing of gait” in Parkinson subjects [11]. Electronic devices equipped with three-axis accelerometers can be employed measuring these kinds of alterations [10]. These measurement systems should be able to record the acceleration on three axes—x , y , and z , store data in memory, and send them to a computer [12], [13]. Furthermore, accelerometers can be used to evaluate the efficacy of therapy procedures in Alzheimer [14] and Parkinson [15], [16] subjects.
Sometimes, in addition to these physical alterations, patients suffer from mental disorders such as memory impairment and dementia. In such cases, the best choice is the employment of wearable systems that are able to monitor movements’ quality and, at the same time, track the patients’ position through a GPS receiver. With such systems, it is possible to record movement anomalies even over long distance.

The monitoring system here presented has several of the above desirable features: it is wearable, it is able to record, store, and wirelessly transmit three-axial acceleration data, and it can track the GPS position of the patient wearing it. Furthermore, it can be developed with less than U.S. $80; it could be effectively used for monitoring patients affected by neurodegenerative diseases, under the medical supervision, both for indoor (hospital) and outdoor (telemedicine) applications.

II. System Development and Validation

The developed system is based on the LinkitONE prototyping board connected to an array of four accelerometers (ADXL345 by Analog Device) through a connection board designed and fabricated by the authors. Considering the frequency range of movement disorders and the need to keep the overall price low, MEMS accelerometers were used instead of piezoelectric devices. The three-axis ADXL345 is a MEMS device, small and ultralow power, suitable for portable applications. It includes a 13-bit analog-to-digital converter (ADC) and allows measurements in the range of ±157 m/s^2. The digital output data can be sent via SPI (3/4 wire) or I2C communication interface. The LinkitONE board is also equipped with a GPS receiver so that the acquired data can be georeferenced and sent via Bluetooth, Wi-Fi, or GSM protocol.
The board is based on the ARM7 EJ-S MediaTek MT2502 (Aster) system-on-chip, with 260-MHz system clock, 4-MB RAM memory, 16 MB of the storage flash memory, and an SD card slot for external additional memory. The board also includes GSM, GPRS, Bluetooth (2.1 and 4.0), and Wi-Fi transceivers. The used communication protocol depends on the external device connected (PC, tablet, and smartphone), and it can be selected by means of a cross-platform interface developed in Java.

Several connection protocols allow handling different application scenarios.

1. The Bluetooth connection is employed between the system and a notebook/tablet for laboratory/medical tests in real time with medical personnel in the same room of the monitored subject.

2. The Wi-Fi connection allows more compact employment for people at home owning Wi-Fi facilities. Both in the first and second cases, data can be stored in a cloud via Wi-Fi.

3. In open scenario applications, the data can be sent to a remote supervisor by GSM protocol.

4. The GPS protocol is employed for the geotagging of the patient. This can be useful for Alzheimer subjects (e.g., in cases of dementia). These data can be sent by the GSM protocol.

A block diagram of the system is reported in Fig. 1.

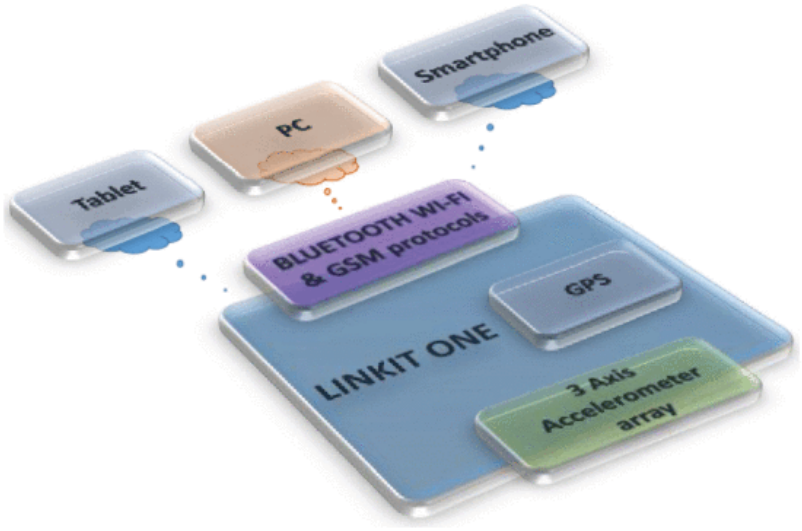

Fig. 1. Block diagram of the monitoring system.

The computer software was developed in Java environment using a multithread approach. It collects data from our system via Bluetooth and plots the results in a graphical user interface. The software allows to set the sampling period and to select the number of sensors needed for measurement. Often a single accelerometer is enough for tremor monitoring, sometimes three or more accelerometers are needed, for example, in the evaluation of the hand tremor [17], [18]. The device is equipped with a long-life battery (3.8 V, 5.1 Ah) so that

it can be used to monitor patients outdoor. The average supply current for the device is 60 mA, and with a single charge, the prototype can be used for about 48 h.

Alternatively, it is possible to use the device in the Wi-Fi mode, the network architecture is shown in Fig. 2. In this case, the board connected to a Wi-Fi network is able to collect the data from the patient, elaborate them, and send them to a server. The patient or a doctor can easily access this server through the developed web app, shown in Fig. 3, in which all the data acquired are plotted in real time, and some statistics are given.

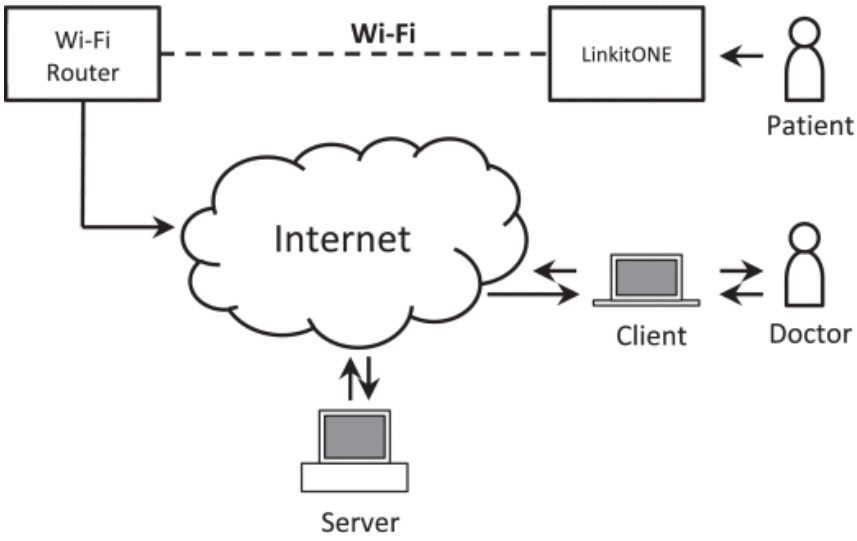

Fig. 2. Network architecture when the Wi-Fi mode is selected.

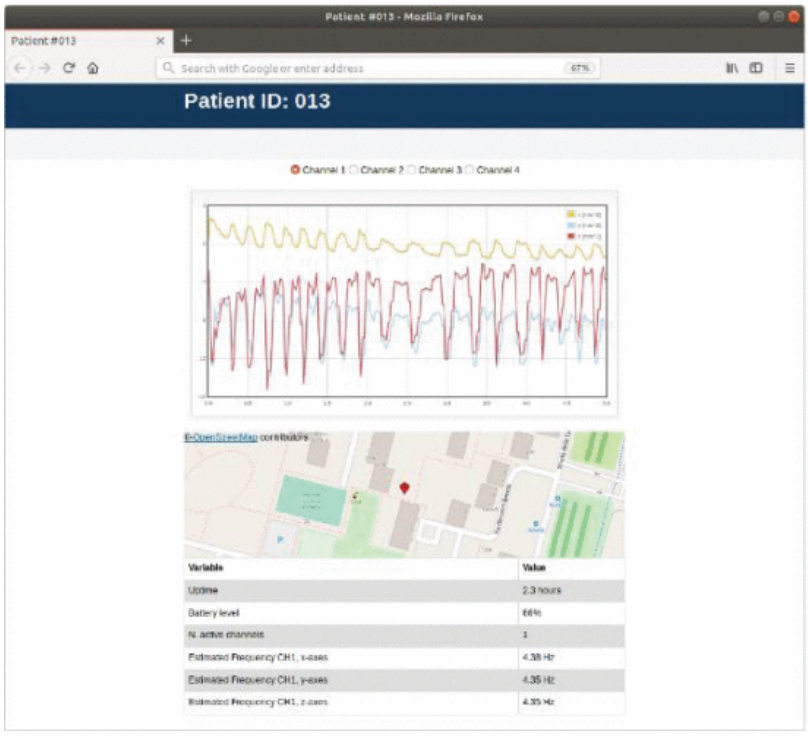

Fig. 3. Developed web app: it consists of a web page that shows all signals in real time and provides devices information and positions.

A 3-D printed polylactic acid case hosts the electronic boards of the system. It has the size of a cigarette packet and was designed and realized in our laboratories with a Renkforce RF1000 3-D printer. Fig. 4 shows the

design of the system and its realization. The four accelerometers can be fixed in different parts of the body in order to monitor the movement quality, as shown in Fig. 5.

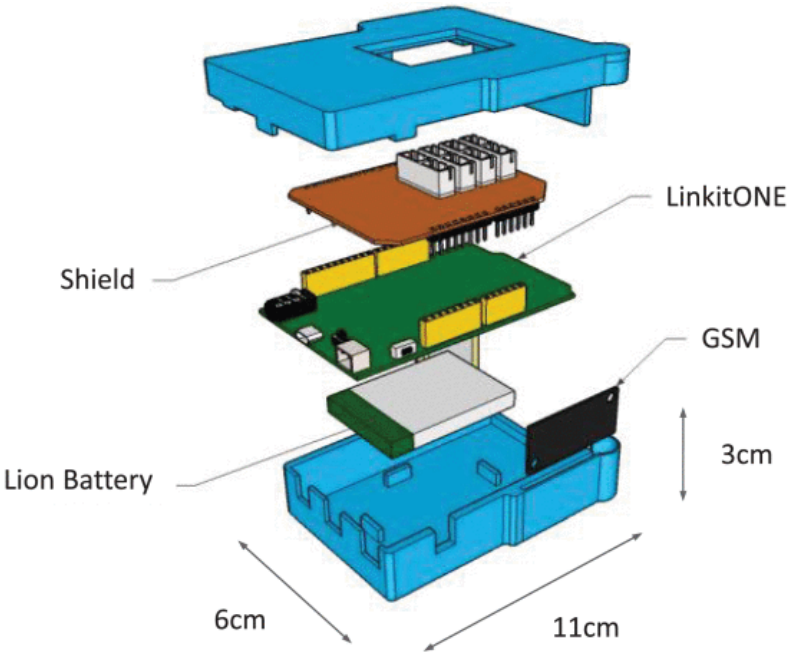

Fig. 4. 3-D design of the enclosure.

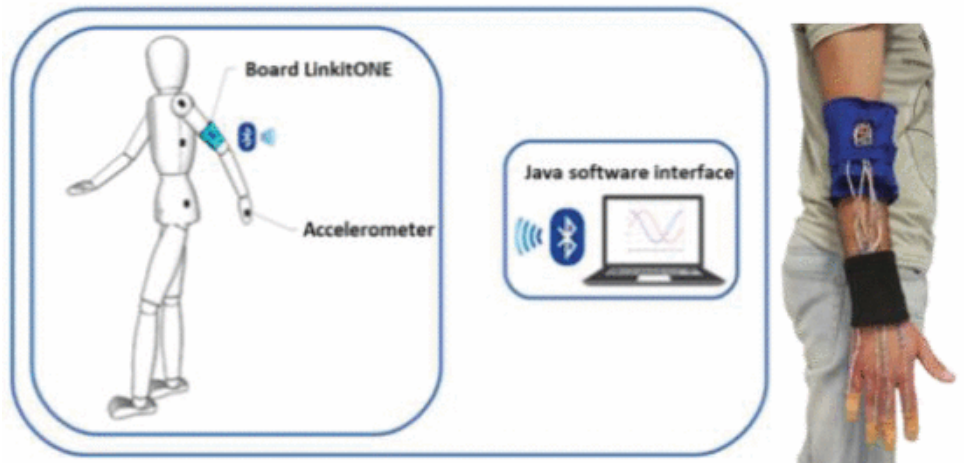

Fig. 5. Wearing the system for tremor measurement.

In order to reduce the amount of data sent to the server from the developed system, a compression algorithm was implemented in the board firmware. The basic idea of this algorithm consists in sending a set of N data $D=\{d_1,\ldots,d_N\}$, in which each value is the difference between a set of samples acquired $X=\{x_1,\ldots,x_N\}$ and the minimum value in this set $\mu=\min\{X\}$. Of course, starting from the set $C=\{\mu,D\}$, it is possible to rebuild the original data set X as $x_i=d_i+\mu$ (with $i\epsilon[1,\ldots,N]$). If data in the set X are correlated, it is possible to demonstrate that the set C can be represented with less bits in comparison to the set X. The whole algorithm and its performance are widely described in [19]. Furthermore, the use of a compression algorithm reduces the power consumption of the wearable system [20], [21].
A few experimental results about the compression algorithm MinDiff, when applied to acceleration signals, are reported in Table I. More precisely, in Table I, we reported the minimum, mean, and maximum compression factors (CFs) of the algorithm, defined here as the ratio between the number of bits before and after compression, that is,

$$\mathrm{CF} = \frac{\text{number of bits BEFORE compression}}{\text{number of bits AFTER compression}}$$

TABLE I
Minimum, Mean, and Maximum CFs for Different Axes

Direction	CF_{min}	CF_{mean}	CF_{max}
X	3.90	4.07	4.35
Y	2.20	2.49	3.04
Z	1.96	2.45	3.07

As it is possible to observe, the average compression ratio in the X -direction is slightly greater than 4, while it approaches 2.5 in the other two directions, i.e., Y and Z . Different results on different axes can be explained considering that in the X -direction, effects of tremors are reduced, and thus, related signals have a lower dynamic; consequently, the compression algorithm is more effective in the X -direction.
Moreover, the board has the basic functions of a cell phone, in particular, it is able to send or receive commands via GSM protocol. For an instance, with a simple text message, it is possible to activate the system remotely and start a new measurement session.

Furthermore, it is possible to query the device about its position and the movement quality. Finally, the system is able to generate and send alarms, messages, or prerecorded calls to another telephone number in case of accidental falls, low battery level, or other dangerous events. The supervisor, in this case, could be a central monitoring and control station for telemedicine.

The ADXL345 accelerometers and the entire system were characterized in a controlled environment with calibrated instruments. The measurement setup included: a signal generator, an amplifier, a linear motion actuator, a laser interferometer for high-accuracy position measurements, and an acquisition system. A schematic of the measurement setup is shown in Fig. 6. The accelerometers were fixed together in a metal block and placed on the linear actuator with an inclination along two axes in order to obtain an equal acceleration component on the *x*-, *y*-, and z -axes. A Keysight 35670A was used to generate a sine wave with a well-defined frequency and its amplitude was selected through an amplifier connected to the linear actuator. The oscillations generated by the actuator were measured through the laser interferometer and acquired with the NI USB-4431 acquisition system.

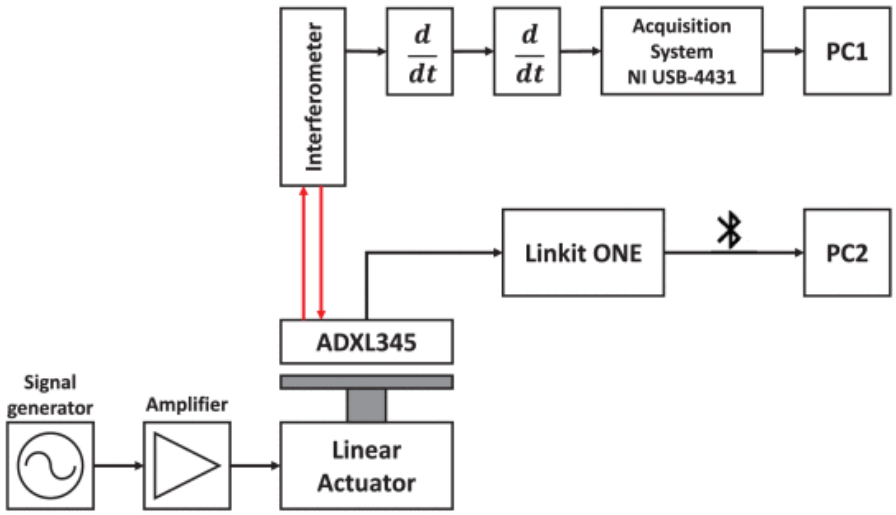

Fig. 6. Schematic of the measurement setup. The laser interferometer and the reference measurement chain are traceable to the national standard.

Part of the measurement setup is shown in Fig. 7. All the accelerometers were subjected to the same input vibrations in a frequency range spanning from 3 Hz up to 10 Hz in eight different steps. Moreover, their response was evaluated at a fixed oscillation frequency and different values of accelerations.

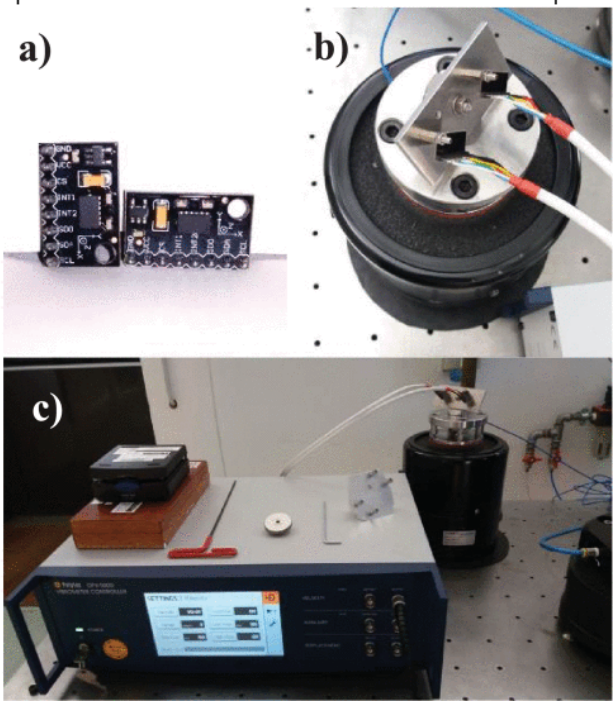

Fig. 7. (a) Two ADXL345. (b) Two accelerometers connected to the same metal block on the linear motion actuator. (c) Part of the measurement setup.

From these experimental measurements, the calibration curve for all the accelerometers was constructed by linear fitting of the input–output relationship (Fig. 8). After the calibration procedure, the overall uncertainty in the acceleration measurement was estimated to be less than 0.5 m/s^2 for all the sensors used. In Figs. 8 and 9, the calibration curves and the calibration fit residual for one of the accelerometers are, respectively, reported. The accelerometer response after the calibration procedure is reported in Fig. 10.

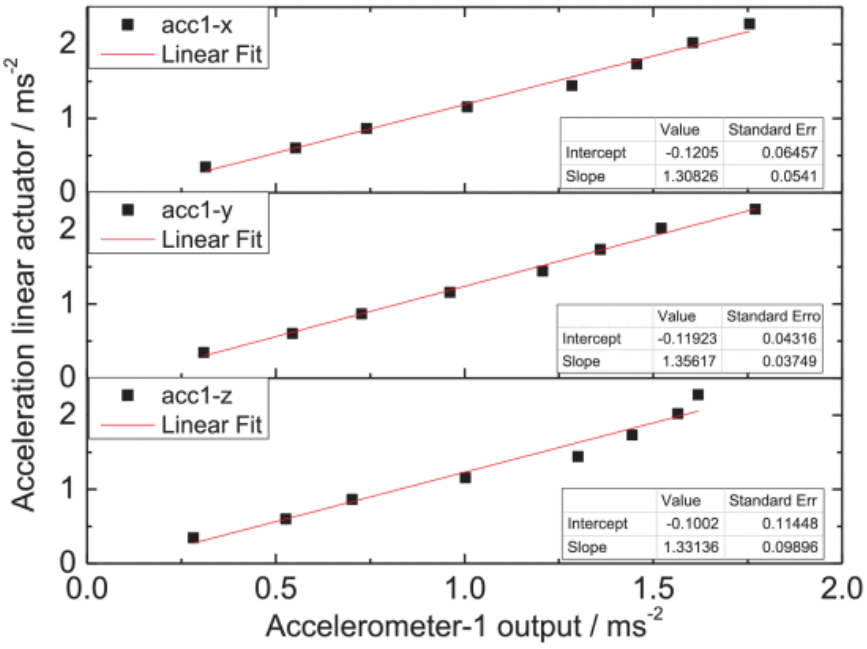

Fig. 8. Calibration curve for accelerometer-1. Zero-offset acceleration (intercept) and the scale factor (slope) are reported in the graph.

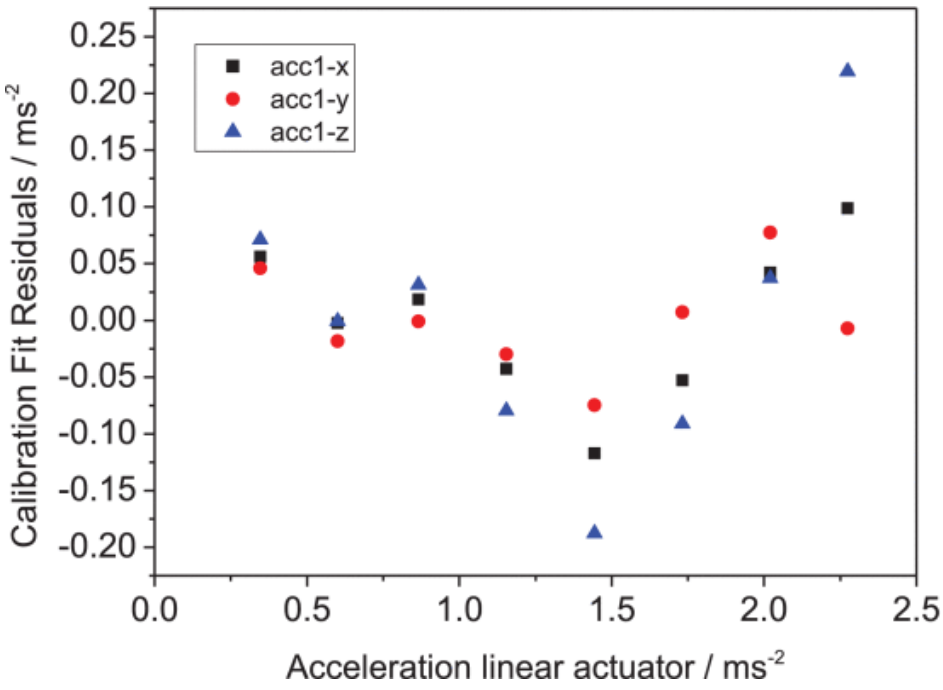

Fig. 9. Calibration fit residual for the x -, y-, and z -axes of accelerometer1.

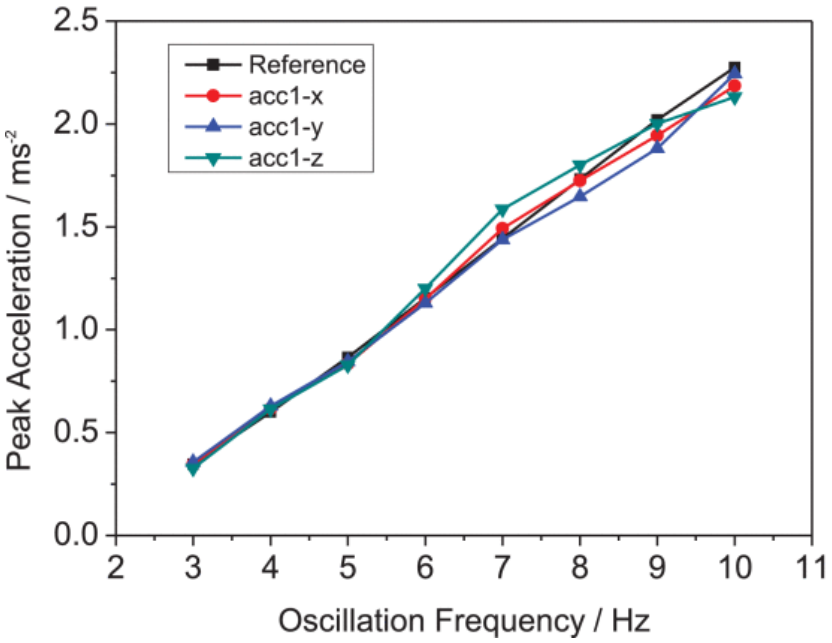

Fig. 10. Comparison between the acceleration reference and the accelerometer-1 output (x -, y -, and z -axes) after calibration at different oscillation frequencies. The accelerometer response, compensated after the calibration procedure, is in a good agreement with the reference for frequencies below 6 Hz. This measurement range is compatible with parkinsonian tremors.

The biomedical signals acquired were processed with a digital low-pass filter. In this paper, we report the implementation of two different digital filters used in our measurements: the finite impulse response (FIR) and the infinite impulse response (IIR) filters, both are implemented and compared. Tables II and III give the design parameters for each filter.

TABLE II
FIR Filter (Design Parameters)

f_t	15 Hz
Δf	2 Hz
$A_s \vert dB$	60 dB
$A_{cf} \vert dB$	3 dB
Coefficients	69
Window	Blackman
f_s	50 Hz

TABLE III
IIR Filter (Design Parameters)

f_t	15 Hz
Δf	2 Hz
$A_s \vert dB$	60 dB
$A_{cf} \vert dB$	3 dB
Filter	Butterworth
Order	5
f_s	50 Hz

IIR filters have low computational cost but their phase response is not linear. On the other hand, FIR filters have higher implementation costs but are stable and have a linear phase response [22]. Usually, linearity is mandatory in the case of biomedical applications, where the information is in the waveform of the signals (e.g., peaks positions in an electrocardiogram signal). Nevertheless, the proposed IIR filter is suitable for our monitoring system. In fact, as shown in Fig. 11 where spectra of IIR and FIR filtered signals are compared, there is a negligible difference below 15 Hz (i.e., for all meaningful frequencies); moreover, as shown in Fig. 12, in the time domain, it is possible to neglect the nonlinearities introduced by the IIR filter (peaks numbers and positions coincide).

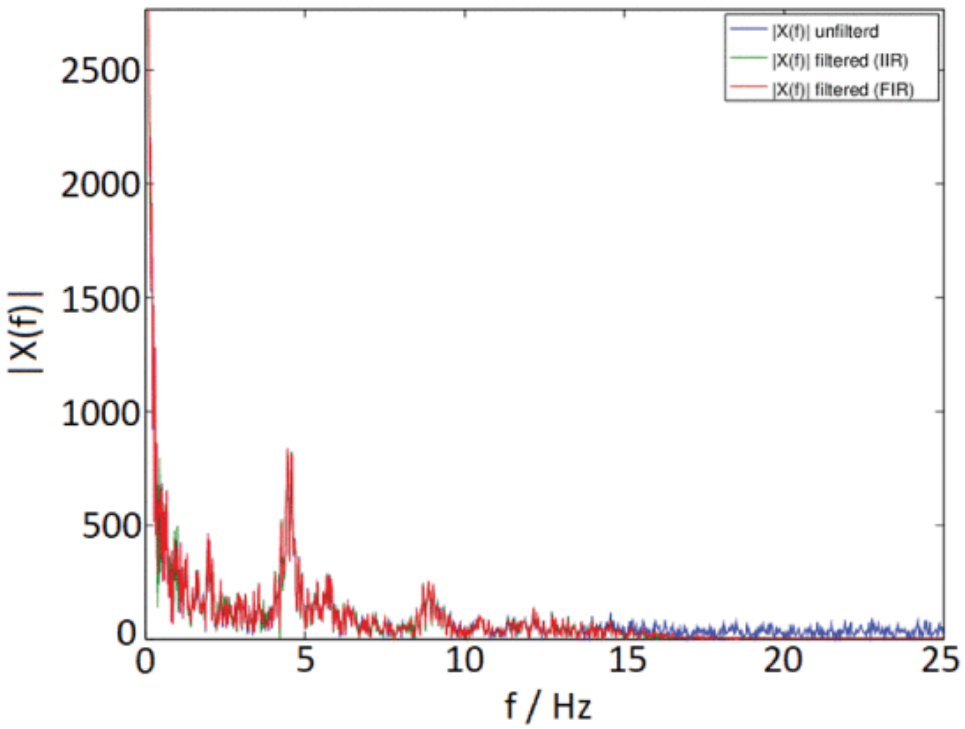

Fig. 11. Comparison of FIR and IIR output signals (x -components) in the frequency domain. The fast Fourier transform (FFT) was computed from raw data coming from the ADC. Both filters have the same cutoff frequency, i.e., 15 Hz.

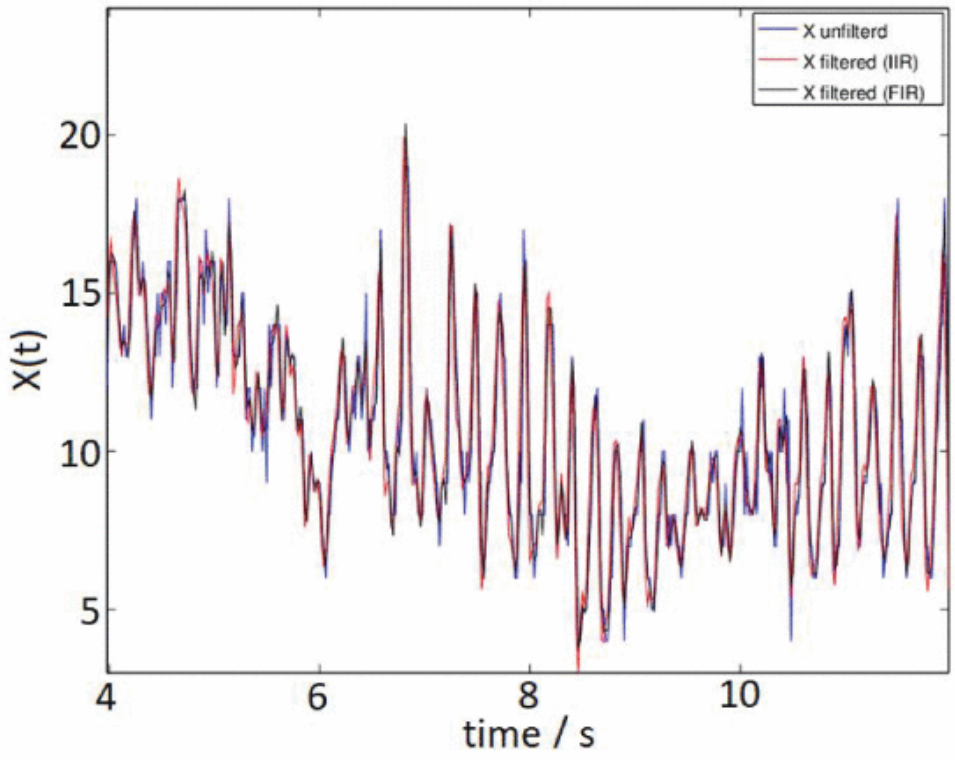

Fig. 12. Comparison of FIR and IIR output signals (x -components) in the time domain (raw data coming from ADC). Even if the phase is not linear in the IIR filter, it is possible to neglect the nonlinearities (peaks numbers and positions coincide).

For portable applications, low computational resource devices are needed, in order to both reduce weight and dimensions, and they are preferable in real-time elaboration of signals coming from several sensors. Thus, the IIR filter implementation seems to be the best choice in our framework since it needs cheap resources providing at the same time high-quality filtered signals. According to [7], digital filters can be integrated into the device

in order to select specific movement contributions for frequency estimation [23] and for filtering noise-affected signals [24].

The features of the device reported in this paper accomplish the main requirements requested for an efficient tremor monitoring system [25].

III. Results

As reported in the literature, the developed system is able to perform frequency measurement procedures in a range suitable with the movement disorders of subjects affected by neurological diseases [26], [27]. Then, it was validated under the medical supervision and here reported results are obtained in the monitoring of the tremors in real subjects. This paper was approved by Local Ethic Committee of IRCCS Centro Neurolesi “Bonino-Pulejo” of Messina (Scientific Institute for Research, Hospitalization, and Health Care).

The group under monitoring is composed of 41 idiopathic parkinsonian subjects admitted at the disorder movement unit of Centro Neurolesi “Bonino-Pulejo” (19 females, 22 males, mean age 70 ± 11.3 years). In this paper, the data regarding two male subjects are reported: a 40-year-old patient suffering from essential tremor (disease duration 5 years) and a 62-year-old patient with idiopathic Parkinson’s disease (PD) (disease duration: 7 years). The first subject did not take drug therapy, while the second was in therapy with levodopa. None of the patients were affected by other neurological, endocrinal, or cardiac diseases. Finally, a 54-year-old woman was also involved in our study as a healthy subject, in order to make a comparison with sick patients.

The first case reported is about the evaluation of the action tremor procedure shown by a subject under muscle contraction. He was asked to wear the system keeping his hand, as shown in Fig. 5, without any further weight, and the tremor was then evaluated. Finally, he was asked to hold a pen with the same hand, and the measurement procedure was performed again. Data were recorded and displayed by mean of the multithread interface developed in Java.

Fig. 13(a) and (b) shows the comparison between two acquisitions for a subject at rest condition and holding a pen, respectively.

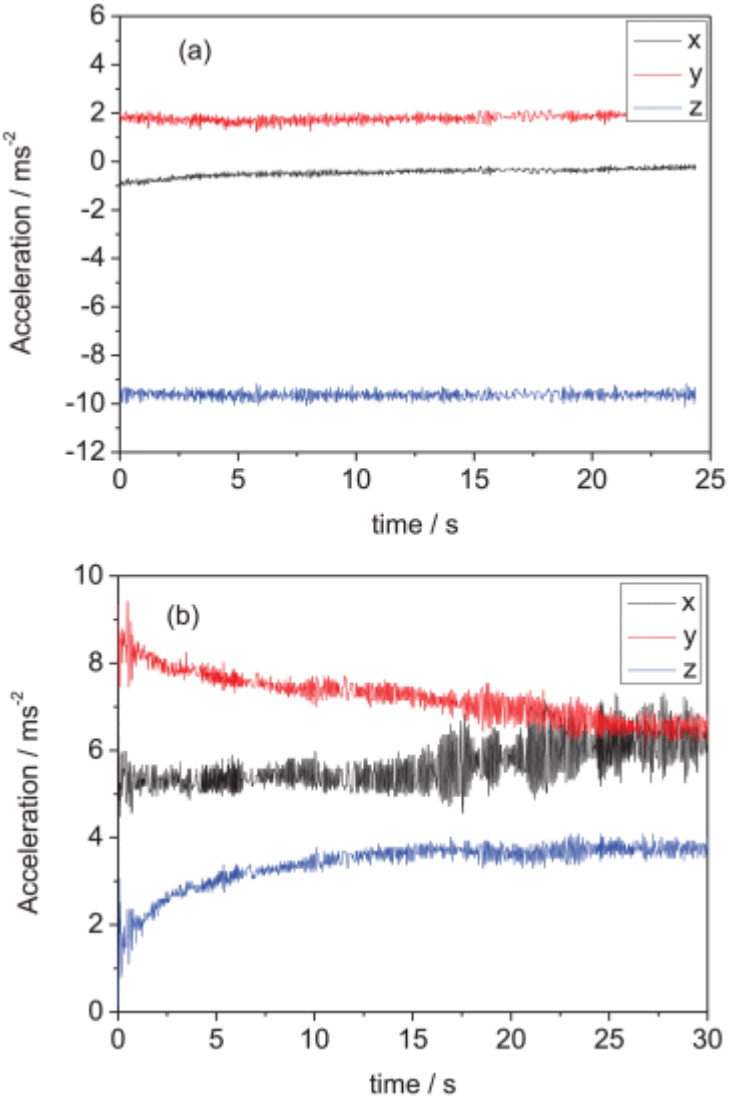

Fig. 13. Action tremor in a real subject. (a) Rest position. (b) Holding a pen. Tremor is recorded only when the muscle is exerting effort.

The second case reported is about a clear Parkinson subject; the measurement procedure was to record tremor data of the hand in two different positions: rest (on a table) and hold (holding in front of the subject). Fig. 14 shows the filtered and the unfiltered movements of the left hand in the hold position; it can be noted how the IIR filter increases the quality of the signal of the x -, y -, and z -axes. All the measurements reported in real cases with specific movements were performed under medical supervision.

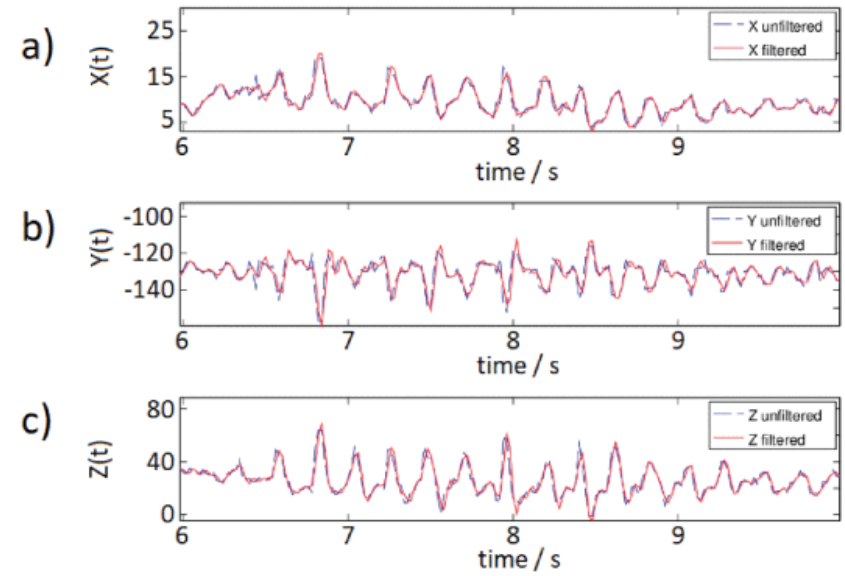

Fig. 14. Recorded tremors of a Parkinson subject in the time domain of the held hand. The three plots report the filtered and unfiltered signals (raw data coming from the ADC) for each axis. (a) x -component. (b) y -component. (c) z -component. There is no distortion in the filtered signal, although an IIR filter was used.

The final case is about a healthy subject, and the related acquisition in the time domain is compared to that of the Parkinson patient (Fig. 15). The signal for the healthy subject has a peak-to-peak value much lower than the signal of the sick patient, and the waveform does not follow a regular pattern. On the other hand, the waveform for the Parkinson subject is close to a sinusoidal signal. This is much more evident in the frequency domain when the healthy subject is compared to sick patients. For the healthy subject, the spectrum, shown in Fig. 16, is almost flat, for the PD subject, a peak close to 5 Hz appears, and for other patients, the tremor frequency is close to 8 Hz.

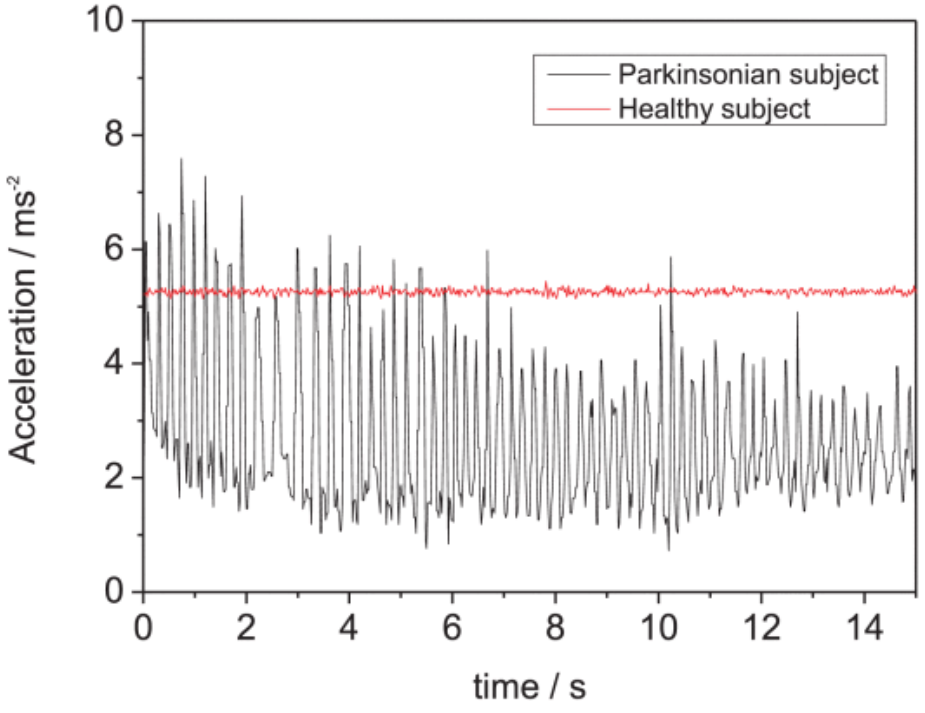

Fig. 15. Comparison between tremor in the parkinsonian subject (black) and healthy subject (red). Acquisition in the time domain, x -component.

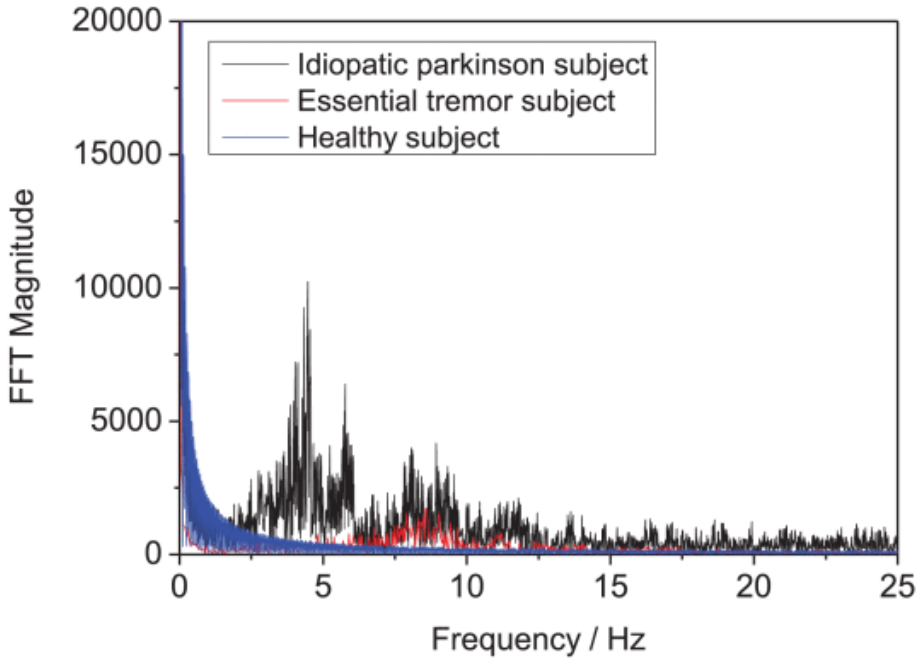

Fig. 16. Spectrum of the acquired signal in idiopathic Parkinson subject (black), essential tremor subject (red), and healthy subject (blue). For a sick patient, the spectrum shows some peaks above 3 Hz. The FFT was computed from raw data coming from the ADC.

Furthermore, if we consider the Unified PD rating scale (UPDRS III), the parkinsonian subject shows the following parameter values (motor subscore): 22; Hoehn and Yahr stage: 1.5.

IV. Conclusion

This paper describes the development of the compact of the high configurable measurement system for movement quality. The system accomplishes the main features required for tremor monitoring devices with a high level of versatility. The data of three subjects were reported through the group under monitoring, which is composed of 41 parkinsonian subjects. The statistical analysis of the whole group is currently under medical evaluation in order to relate the measured data with the UPDRS III. Finally, the signal processing algorithm will be improved with the possibility to recognize a possible parkinsonian candidate or determine a severity index of the disease. In addition, this system could give a contribution to therapeutic management of these patients.

References

1.

F. Mohamedali and N. Matoorian, "Support dementia: Using wearable assistive technology and analysing real-time data", Proc. Int. Conf. Interact. Technol. Games (ITAG), pp. 50-54, Oct. 2016.

2.

F. L. Pagan, "Improving outcomes through early diagnosis of Parkinson's disease", Amer. J. Managed Care, vol. 18, no. 7, pp. S176, Sep. 2012.

3.

G. Gugliandolo et al., "A movement monitoring system for patients of neurodegenerative diseases", Proc. IEEE Int. Instrum. Meas. Technol. Conf, pp. 1-6, May 2018.

4.

C. Godinho et al., "A systematic review of the characteristics and validity of monitoring technologies to assess Parkinson's disease", J. NeuroEng. Rehabil., vol. 13, no. 1, pp. 24, Mar. 2016.

5.

Y. Su et al., "3-D motion system ('data-gloves'): Application for Parkinson's disease", IEEE Trans. Instrum. Meas., vol. 52, no. 3, pp. 662-674, Jun. 2003.

6.

G. V. Kondraske, "A noncontacting human tremor sensor and measurement system", IEEE Trans. Instrum. Meas., vol. IM-35, no. 2, pp. 201-206, Jun. 1986.

7.

A. Bermeo, M. Bravo, M. Huerta and A. Soto, "A system to monitor tremors in patients with Parkinson's disease", Proc. 38th Annu. Int. Conf. IEEE Eng. Med. Biol. Soc. (EMBC), pp. 5007-5010, Oct. 2016.

8.

L. Li et al., "Multi-sensor wearable devices for movement monitoring in Parkinson's disease", Proc. 8th Int. IEEE/EMBS Conf. Neural Eng. (NER), pp. 70-73, Aug. 2017.

9.

J. Szurley and C. Druzgalski, "A novel approach in remote monitoring and assessment of patient balance", Proc. Pan Amer. Health Care Exchanges, pp. 143, Mar. 2009.

10.

B. Andó et al., "A wearable device to support the pull test for postural instability assessment in Parkinson's disease", IEEE Trans. Instrum. Meas., vol. 67, no. 1, pp. 218-228, Jan. 2018.

11.

C. Punin et al., "Wireless system for detection of FOG in patients with Parkinson's disease", Proc. Global Med. Eng. Phys. Exchanges/Pan Amer. Health Care Exchanges (GMEPE/PAHCE), pp. 1-4, Jul. 2017.

12.

A. Tay et al., "Real-time gait monitoring for Parkinson disease", Proc. 10th IEEE Int. Conf. Control Automat. (ICCA), pp. 1796-1801, Jul. 2013.

13.

R. LeMoyne, C. Coroian and T. Mastroianni, "Quantification of Parkinson's disease characteristics using wireless accelerometers", Proc. ICME Int. Conf. Complex Med. Eng., pp. 1-5, May 2009.

14.

Y. L. Hsu et al., "Gait and balance analysis for patients with Alzheimer's disease using an inertial-sensor-based wearable instrument", IEEE J. Biomed. Health Inform., vol. 18, no. 6, pp. 1822-1830, Nov. 2014.

15.

S. Askari, M. Zhang and D. S. Won, "An EMG-based system for continuous monitoring of clinical efficacy of Parkinson's disease treatments", Proc. Annu. Int. Conf. IEEE Eng. Med. Biol., pp. 98-101, Sep. 2010.

16.

J. Barth et al., "Biometric and mobile gait analysis for early diagnosis and therapy monitoring in Parkinson's disease", Proc. Annu. Int. Conf. IEEE Eng. Med. Biol. Soc., pp. 716-868, Sep. 2011.

17.

Y. Zhou, M. E. Jenkins, M. D. Naish and A. L. Trejos, "The measurement and analysis of parkinsonian hand tremor", Proc. IEEE-EMBS Int. Conf. Biomed. Health Inform. (BHI), pp. 414-417, Feb. 2016.

18.

J. van den Nooet et al., "Applications of the powerglove for measurement of finger kinematics", Proc. 11th Int. Conf. Wearable Implantable Body Sensor Netw. Workshops, pp. 6-10, Jun. 2014.

19.

G. Campobello, O. Giordano, A. Segreto and S. Serrano, "Comparison of local lossless compression algorithms for wireless sensor networks", J. Netw. Comput. Appl., no. 47, pp. 23-31, Jan. 2015.

20.

K. C. Barr and K. Asanović, "Energy-aware lossless data compression", ACM Trans. Comput. Syst., vol. 24, no. 3, pp. 250-291, Aug. 2006.

21.

G. Campobello, A. Segreto and S. Serrano, "Data gathering techniques for wireless sensor networks", Int. J. Distrib. Sensor Netw., vol. 12, no. 3, pp. 1-17, Mar. 2016.

22.

E. Ifeachor and B. Jervis, Digital Signal Processing: A Practical Approach, Upper Saddle River, NJ, USA:Prentice Hall, 2001.

23.

G. Campobello, G. Cannatá, N. Donato, A. Famulari and S. Serrano, "A novel low-complex and low-memory method for accurate single-tone frequency estimation", Proc. 4th Int. Symp. Commun. Control Signal Process. (ISCCSP), pp. 1-6, Mar. 2010.

24.

M. Galeano, A. Calisto, A. Bramanti, S. Serrano, G. Campobello and B. Azzerboni, "R-point detection for noise affected ECG recording through signal segmentation", Proc. Annu. Int. Conf. IEEE Eng. Med. Biol., pp. 638-641, Sep. 2010.

25.

R. J. Elble and J. McNames, "Using portable transducers to measure tremor severity", Tremor Other Hyperkinetic Movements, vol. 6, pp. 375, May 2016.

26.

H. Dai, P. Zhang and T. C. Lueth, "Quantitative assessment of parkinsonian tremor based on an inertial measurement unit", Sensors, vol. 15, no. 10, pp. 25055-25071, 2015.

27.

B. Carignan, J.-F. Daneault and C. Duval, "Quantifying the importance of high frequency components on the amplitude of physiological tremor", Exp. Brain Res., vol. 202, no. 2, pp. 299-306, Apr. 2010.